Published in final edited form as:
Curr Biol. 2009 December 1; 19(22): 1875–1885. doi:10.1016/j.cub.2009.09.059.

ARF6-regulated shedding of tumor-cell derived plasma membrane microvesicles

Vandhana Muralidharan-Chari[1], **James Clancy**[1], **Carolyn Plou**[1], **Maryse Romao**[2], **Philippe Chavrier**[2], **Graca Raposo**[2], and **Crislyn D'Souza-Schorey**[1,3]

[1]Department of Biological Sciences, University of Notre Dame, Notre Dame, USA

[2]Institut Curie, Centre de Recherche, Paris, F-75248 France

Abstract

Background—Increased MAPK signaling, small GTPase activation, cytoskeletal rearrangements and the directed targeting of proteases to sites of extracellular matrix degradation, all accompany the process of tumor cell invasion. Several studies have implicated the small GTP-binding protein, ARF6, in tumor cell invasion although the molecular basis by which ARF6 facilitates this process is unclear.

Results—We show that the ARF6 GTP/GDP cycle regulates the release of protease-loaded plasma membrane-derived microvesicles from tumor cells into the surrounding environment. To enable microvesicle shedding, ARF6-GTP dependent activation of phospholipase D promotes the recruitment of the extracellular signal-regulated kinase (ERK) to the plasma membrane where in turn, ERK phosphorylates and activates myosin light chain kinase (MLCK). MLCK-mediated MLC phosphorylation is required for microvesicle release. Inhibition of ARF6 activation is accompanied by PKC-mediated phosphorylation of MLC, which blocks microvesicle shedding. Protein cargo appears to be selectively sorted into microvesicles and adhesion to the ECM is facilitated by microvesicle-associated integrin receptors.

Conclusions—Microvesicle shedding in tumor cells occurs via an actomyosin-based membrane abscission mechanism that is regulated by nucleotide cycling on ARF6. Microvesicle shedding appears to release selected cellular components, particularly those involved in cell adhesion and motility, into the surrounding environment. These findings suggest that ARF6 activation and the proteolytic activities of microvesicles both of which are thought to correlate directly with tumor progression, could potentially serve as biomarkers for disease.

INTRODUCTION

Metastasis, a life-threatening hallmark of cancer, occurs when cells detach from the primary tumor and 'invade' surrounding tissues to reach distal locations[1]. Growth factor induced signaling, cytoskeletal rearrangements mediated by the Rho-family GTPases and alterations to adhesive and migratory potential of cells, all accompany the process of cell invasion [2]. Furthermore, proteases from all four classes (serine, cysteine, aspartic, and

[3]Correspondence should be addressed to: Crislyn D'Souza-Schorey, Department of Biological Sciences, University of Notre Dame, Box 369, Galvin Life Sciences Building, Notre Dame, IN 46556-0369. cdsouzas@nd.edu.

metalloproteases) have been implicated in ECM degradation and their expression, activation and secretion are vital for tumor cell invasion [3].

Over the past few years, ARF6, of the ARF family of small GTP-binding proteins, has emerged as an important signaling molecule and has been shown to regulate membrane trafficking and actin cytoskeleton remodeling, both of which can impinge on the acquisition of migratory/invasive potential (reviewed in [4]). Recent studies utilizing *in vitro* cell invasion assays have indicated that in invasive melanoma, glioma, and breast cancer cell lines, the ARF6 GTP/GDP cycle can regulate invasive potential [4]. Cellular depletion of ARF6 by siRNA or inhibition of ARF6 activation by expression of a dominant negative ARF6 mutant attenuates tumor cell invasion *in vitro*. Recent studies in animal models have also revealed a vital role for ARF6 activation in melanoma and glioma cell invasion [5, 6]. Moreover, screening of various breast tumor cell lines reveal a direct correlation between ARF6 protein expression and invasive capacity [7]. Finally, the ARF6 exchange factor GEP100, was expressed in 70% of primary breast ductal carcinomas, and was preferentially co-expressed with EGFR in malignant tumors [8].

What might be the cellular basis by which ARF6 promotes cell invasion? First, ARF6 has been implicated in regulation of invadopodia turnover [4]. Second, via its effects on membrane traffic and remodeling, ARF6 could regulate protease secretion. The current study focuses on the role of ARF6 in protease release. We show that via its effects on phospholipid metabolism and ERK activation, ARF6 regulates protease release by modulating the shedding of plasma membrane-derived microvesicles into the surrounding environment. Vesicle shedding by the outward fission of membrane vesicles from the cell surface is a selective process that occurs in a spectrum of normal and more frequently in tumor cells, both *in vivo* and *in vitro* [9]. These released microvesicles (also referred to as microparticles, particles and ectosomes) have been widely detected in various biological fluids including peripheral blood and in ascitic fluids; their composition depends on the cells from which they originate [10, 11]. They are thought to facilitate cell invasion, evasion of the immune response, bone mineralization, and even tumor cell intravasation by reducing cell size [12]. Here we provide structural and biochemical characterization of ARF6-positive microvesicles shed by tumor cells. We also show that protease cargo contained within the microvesicles is functionally robust and promotes matrix degradation. Finally, we delineate the pathway by which ARF6 maneuvers the actomyosin machinery to facilitate shedding of microvesicles from the tumor cell surface. These findings are significant particularly in light of reports demonstrating that proteolytic activities of microvesicles shed by tumor cells correlate directly with malignancy and invasiveness [13, 14].

RESULTS

Phenotypic variations of LOX$^{ARF6\text{-}GDP}$ and LOX$^{ARF6\text{-}GTP}$ cell lines

To investigate mechanisms by which ARF6 promotes cell invasion, we made use of LOX$^{ARF6\text{-}GTP}$ and LOX$^{ARF6\text{-}GDP}$ cell lines that stably express either a HA-tagged, GTPase deficient mutant of ARF6, ARF6-Q67L, or the dominant negative ARF6 mutant, ARF6-T27N, respectively. The most striking phenotype observed upon microscopic examination of LOX$^{ARF6\text{-}GDP}$ cells was the presence of vesicle-like bulbous structures that decorate the cell surface (figure 1A, B). These structures were also seen on the surfaces of LOX and LOX$^{ARF6\text{-}GTP}$ cell lines (figure 1A, B), although they were less readily obvious. Instead, in the latter two cell lines, vesicles were released into the growth medium (figure 1B). The lack of vesicles in the growth media of LOX$^{ARF6\text{-}GDP}$ cells suggests that ARF6 activation is likely required for their release. When collected by low speed centrifugation of the growth media and examined for total protein or probed for ARF6 expression, vesicles shed from LOX$^{ARF6\text{-}GTP}$ cells exhibit significantly more protein and ARF6 indicative of increased

shedding from these cells relative to the parental cell line (figure 1 C). Furthermore, mutant ARF6-GDP was not present on shed vesicles.

The release of vesicles was not as apparent in earlier investigations when LOX cells were seeded on gelatin matrix [15] presumably because they were released into the matrix at the sites of cell invasion. In addition, their detection could have been hampered due to low efficiency of transient transfection used in the previous study. In this study however, upon careful examination of $LOX^{ARF6\text{-}GTP}$ cells on gelatin-coated coverslips, we were able to detect the presence of vesicles in the matrix on the cell surface (figure 1D). Furthermore, as shown in figure 1D-upper panel, these vesicular structures appear to be distinct from cortactin-positive invadopodia that extend into the gelatin matrix. Vesicles do not contain cortactin although they label for β1 integrin (figures 1D, also see figure 4B), which is also present in invadopodia [16]. Quantitation of cortactin label in vesicle relative to invadopodia is shown in figure S1. Some cells exhibit expansive membrane arbors decorated with microvesicles (see figure 1D, middle panel). Cells had a tendency to adopt this arborization phenotype suggestive of horizontal movement when the underlying gelatin is relatively thick (≥ 5 m). It is possible that cells form invadopodia at the adherent face initially and when they invade into 'substantial' matrix and move laterally this arbor phenotype takes effect. In contrast, $LOX^{ARF6\text{-}GDP}$ cells appear bulbous when plated on gelatin largely due to vesicles studded at the cell surface and little to no matrix degradation underneath the cells (figure 1D, lower panel). As reported previously, invadopodia protrusions at the adherent surface were not observed upon expression of the dominant negative ARF6 mutant [15]. Thus ARF6 activation is coupled to two apparently distinct cellular processes linked to matrix invasion, invadopodia formation and the release of surface vesicles into the surrounding environment. In this study, we focus on mechanisms underlying ARF6-regulated vesicle shedding from the tumor cell surface.

Morphological examination of $LOX^{ARF6\text{-}GTP}$ and $LOX^{ARF6\text{-}GDP}$ cell lines using electron microscopy (EM) suggests that vesicles at the surface of cells are heterogeneous in size (300–900 nm) (Figure 1E). EM-based investigations also indicate that cells display no signs of nuclear fragmentation or apoptosis. All of the above suggests that the ARF6 GTPase cycle regulates the release of a heterogeneous population of vesicles from tumor cells into the surrounding environment.

We also examined vesicle shedding in other tumor cell lines; SW480, a colon carcinoma cell line, PC3, a prostate adenocarcinoma cell line and MDA-MB-231, an invasive breast tumor cell line. Gross morphological examination by phase contrast microscopy showed that shed vesicles were present in the growth media of all aforementioned cell lines (data not shown). Analysis of shed vesicles collected from the growth media by immunoblotting revealed the presence of endogenous ARF6 on isolated vesicles (figure 1F). Furthermore, dominant inhibition of ARF6 function by expression of ARF6(T27N) in these tumor cell lines prevented vesicle release (data with SW480 cell line is shown in figure S2).

ARF6-GTP facilitates the release of plasma membrane-derived 'microvesicles' into the surrounding environment

There is accruing evidence for the existence of unconventional secretory mechanisms, such as the release of exosomes and microvesicles that do not utilize the classical signal-peptide secretory transport pathway. Exosomes are internal vesicles of multivesicular bodies/late endosomes that are released upon exocytosis [17]. Morphological characterization of ARF6-regulated shed vesicles suggests that they are 'microvesicles' and henceforth they are referred to as such. Isolated ARF6-positive vesicles pellet by centrifugation at approximately 10,000g, unlike exosomes that sediment by centrifugation at approximately 100,000g (figure 2A). Figure 2A shows that ARF6-positive vesicles are not present in the

100,000g fraction. Ultrastructural analyses of whole mount preparations of the 10,000g and 100,000g fractions confirmed the heterogeneity of the 10,000g microvesicles relative to the more uniform 50–70nm vesicles characteristic of exosomes in the 100,000g fraction (figure 2B).

Studies have shown that PS (phosphatidylserine) externalization accompanies shedding of plasma membrane-derived microvesicles [11]. Indeed we found externalization of PS on the surface of microvesicles based on reactivity with Annexin-V, a high affinity PS-binding protein. This was particularly evident in $LOX^{ARF6\text{-}GDP}$ cells where microvesicles stud the cell surface (figure 2C). We also note that these microvesicles are not apoptotic bodies. As stated above, expression of ARF6 mutants in LOX cells does not induce morphological changes such as condensed chromatin and pyknotic nuclei or label for cleaved caspase 3. On the other hand, when treated with okadaic acid, a known inducer for apoptosis, a higher proportion of cells label for cleaved caspase 3 (figure 2D). Thus, ARF6 activation facilitates the release of microvesicles.

Shed microvesicles contain proteases and facilitate ECM degradation

Previous reports have shown that microvesicles shed by breast carcinoma and ovarian cancer cell lines contain proteases like MMP-2 and MMP-9 [18]. We find that ARF6-positive microvesicles from the 10,000g fraction contained high and low molecular weight gelatinases as indicated by gelatin zymography (figure 3A) and MT1MMP (figure 4B). Of note, MT1MMP silencing significantly decreased the basal invasiveness in parental LOX cells (our unpublished observations). Moreover, shed vesicles when seeded on FITC-gelatin, were capable of matrix degradation that appeared as dark spots around microvesicle membranes (figure 3B).

It has been proposed that β1 integrins facilitate interaction of shed microvesicles with the ECM and that vesicle contents are released after microvesicle burst induced by acidic pH characteristic of the tumor environment [19]. We have found that addition of inactivating β1 integrin antibody, AIIB2, to isolated microvesicles (figure 3B) or LOX cells (not shown), blocked adhesion and matrix degradation, suggesting that protein topology in the microvesicle membrane is still maintained and that integrin receptor association with matrix is important for microvesicle-mediated matrix degradation. AIIB2 also labels the extracellular surface of cells and shed microvesicles (figure 3C). Thus, while proteases at the invadopodia surface facilitate local pericellular proteolysis, microvesicle release could provide a mechanism for rapid and directed proteolysis at distal sites creating paths of less resistance.

Selective sorting of cargo into cell surface microvesicles

Besides proteases, microvesicles have been shown to be selectively enriched in β1 integrin receptors and MHC class I molecules. Both MHC class I molecules and integrin receptors traffic to and from the plasma membrane via ARF6-regulated endosomal compartments [20]. Figure 3D shows labeling for MHC class 1 in $LOX^{ARF6\text{-}GDP}$ cells in the perinuclear compartments and the cell surface, but largely at the cell surface in $LOX^{ARF6\text{-}GTP}$ cells. Western blotting analysis of shed vesicles revealed that along with endogenous ARF6, MHC-I, β1 integrin, VAMP 3 and MT1-MMP were also present in microvesicles (figure 3E). Of note, processed forms of MT1-MMP are present in the microvesicles. However, microvesicles were devoid of transferrin receptors, VAMP7 or Rab8A and known components of invadopodia, cortactin and Tks5. Thus, cargo trafficked via recycling endosomes to the cell surface appears to be selectively sorted into these surface microvesicles.

ARF6-GTP-induced microvesicle shedding requires the extracellular signal regulated kinase (ERK)

ARF6-enhanced melanoma cell invasion is dependent on the activation of the extracellular signal-regulated kinase (ERK) [15]. Moreover the ARF6 GTPase cycle regulates ERK activation[15, 21, 22] downstream of c-Raf /A-Raf[23]. Therefore, we investigated if ARF6-GTP-induced microvesicle shedding is also dependent on ERK signaling. Treatment of LOX and $LOX^{ARF6\text{-}GTP}$ cells with U0126, an inhibitor of MEK, the kinase immediately upstream of ERK, resulted in significant inhibition of basal as well as ARF6-GTP enhanced microvesicle shedding (figure 4A). Upon MEK inhibition, both parental LOX and $LOX^{ARF6\text{-}GTP}$ accumulated microvesicles at the cell surface that resembled the $LOX^{ARF6\text{-}GDP}$ phenotype (figure 4B). Similarly MEK inhibition also blocked microvesicle shedding from PC3 and SW480 cell lines (supplemental figure 3). Thus ARF6-regulated microvesicle shedding requires ERK.

Consistent with earlier findings in HeLa cells [21] we find that ERK localizes to the cytoplasm in $LOX^{ARF6\text{-}GDP}$ cells (figure 4C). In contrast, membrane-associated ERK is predominantly at the cell surface in LOX and $LOX^{ARF6\text{-}GTP}$ cells. This becomes further evident in sub-cellular fractionation studies, wherein the activated phospho-ERK distribution is significantly more in the membrane fraction of $LOX^{ARF6\text{-}GTP}$ cells (figure 4D). Thus ARF6 activation likely enhances ERK redistribution to the plasma membrane, which in turn facilitates its phosphorylation and microvesicle release.

ARF6-regulated ERK activation requires phospholipase D

Studies have shown that ARF6 simulates phospholipase D (PLD) activity [4]. Further, PLD has been shown to facilitate ERK activation. Here, we tested the hypothesis that ARF6 regulated PLD activity is required for ERK activation. First, we examined phospho-ERK levels upon PLD inactivation. We found that expression of ARF6-N48I, an ARF6 mutant defective in PLD activation, inhibits ERK activation (figure 5A) and microvesicle shedding (figure 5B). PA levels were significantly decreased in ARF6-N48I expressing cells (figure 5C) and ERK distribution was in intracellular cytoplasmic structures (figure S4). Next, we used primary alcohols to inhibit PLD, which results in the formation of phosphatidylalcohol at the expense of phosphatidic acid by replacing water. We found that treatment of cells with 1-butanol also inhibits ERK activation (data not shown) and microvesicle shedding (figure 5D). Thus, PLD activation is upstream of ERK activation and is essential for ARF6-regulated microvesicle shedding.

Next, we investigated if we could rescue the shedding of microvesicles in $LOX^{ARF6\text{-}GDP}$ cells by restoring phospho-ERK levels, or by stimulating PLD activity by pathways independent of ARF6. Treatment with propranolol, a PA phosphohydrolase inhibitor [24], restored phospho-ERK levels in $LOX^{ARF6\text{-}GDP}$ cells, as shown in figure 5E and induced microvesicle shedding in $LOX^{ARF6\text{-}GDP}$ cells (figure 5F). Unlike propranolol, another GCPR antagonist, atenolol, did not have any effect on phospho-ERK levels or microvesicle release (figure 5E,F). These data corroborate the importance of PLD and ERK activation in regulating microvesicle shedding. Finally, we determined the effect of 1-butanol on microvesicle shedding induced by expression of constitutively activated MEK. Activated MEK increases microvesicle shedding more than 12-fold compared to the parental LOX cells; however, 1-butanol had little to no effect on microvesicle shedding, confirming that ERK lies downstream of PLD activation (data not shown).

ERK facilitates microvesicle shedding by phosphorylating myosin light chain

Treatment of LOX cells with blebbistatin, a small molecule inhibitor of myosin II activity, or with latrunculin A, an actin-binding toxin that inhibits actin polymerization, profoundly

affected the microvesicle release. In the presence of blebbistatin, microvesicles do not form (figure 6A). 85–90% of latrunculin A treated cells exhibited clustered microvesicles at the cell surface (figure 6A). Accordingly, latrunculin A treatment also inhibited the release of microvesicles from both parental LOX and $LOX^{ARF6\text{-}GTP}$ cells (figure 6B). Thus vesicle shedding is likely mediated via an actomyosin-dependent mechanism. MLCK, a Ca^{2+}/calmodulin-dependent kinase, phosphorylates myosin II light chain (MLC) to promote contraction of the actin-based cytoskeleton[25]. ERK has been shown to phosphorylate MLCK, which in turn phosphorylates MLC at Thr18/Ser19 and thereby stimulates MLC activity, [26, 27]. We tested the hypothesis that ARF6-GTP-induced ERK activation at sites of vesicle release leads to localized activation of MLCK, which in turn stimulates serine phosphorylation of MLC to allow force generation required for microvesicle fission. In support of this contention, immunofluorescent labeling of LOX tumor cells revealed that phospho-MLC localizes to the 'necks' of microvesicles at the cell surface (figure 6C).

We examined phosphorylation of MLC in parental LOX and LOX mutant lines by western blotting. As shown in figure 6D, levels of phospho-MLC are significantly increased in $LOX^{ARF6\text{-}GTP}$ cells compared to parental LOX cells. Treatment of parental LOX and $LOX^{ARF6\text{-}GTP}$ cells with ML-7, an MLCK inhibitor, blocks MLC phosphorylation as well as microvesicle shedding (figure S5). Taken together these data show that ARF6 facilitates microvesicle fission via a mechanism that involves ERK-dependent MLC phosphorylation.

As seen in figure 6D and contrary to our expectations, no decrease in phospho-MLC levels was observed in $LOX^{ARF6\text{-}GDP}$ cells and in fact they were slightly higher than basal levels. A possible explanation for this observation is that the phosphorylation of MLC in $LOX^{ARF6\text{-}GDP}$ cells is 'inhibitory' and independent of ERK. To investigate this further, we compared the levels of phospho-MLC in the presence and absence of U0126 in parental LOX and LOX mutant lines. As seen in figure 6E, inhibition of phospho-MLC was evident in the presence of MEK inhibitor in parental LOX and in $LOX^{ARF6\text{-}GTP}$ cells, but there was no inhibition in phospho-MLC levels in $LOX^{ARF6\text{-}GDP}$ cells. Also, treatment with ML7 had little to no effect on MLC phosphorylation in $LOX^{ARF6\text{-}GDP}$ cells (figure S5). This further confirms that the phosphorylation of MLC in $LOX^{ARF6\text{-}GDP}$ cells is not mediated by ERK.

We examined alternative pathways such as the activation of PKC or p38[28, 29] for MLC phosphorylation in $LOX^{ARF6\text{-}GDP}$ cells. To distinguish between PKC- and p38-mediated phosphorylation of MLC, $LOX^{ARF6\text{-}GDP}$ cells were treated with SB203580, a p38 inhibitor or Go6976, a PKC inhibitor. We found that phospho-MLC levels were decreased specifically upon PKC inhibition (figure 6F). Thus, MLC phosphorylation in $LOX^{ARF6\text{-}GDP}$ occurs via PKC and is independent of phospho-ERK. We also note that MLC phosphorylation is independent of PKC in parental LOX and in $LOX^{ARF6\text{-}GTP}$ cells, as no decrease in phospho-MLC levels was observed in the presence of PKC inhibitor (figure S4). Thus, in $LOXA^{RF6\text{-}GDP}$ cells MLC is phosphorylated by PKC, which is inhibitory, while in $LOX^{ARF6\text{-}GTP}$ cells, MLC phosphorylation is regulated upstream by ERK, a step that promotes MLC-regulated contraction, and in turn, microvesicle fission (see figure 7). Pertinent to these findings, is that PKC-mediated MLC phosphorylation has been documented to decrease MLC activity. In this regard, slow stretch of the canine basilar artery is accompanied by the triphosphorylation of myosin light chain (MLC_{20}) at Thr^{9}, Thr^{18}, Ser^{19} which results in the inhibition of myogenic contraction and thereby, muscle relaxation [30]. In sum, ARF6-GTP facilitates microvesicle fission via a mechanism that involves ERK-dependent MLC phosphorylation and ARF6-GDP has the opposite effect via PKC-induced phosphorylation of MLC.

DISCUSSION

Microvesicle-mediated release of proteases is an important but understudied area of tumor cell biology. Our studies demonstrate that ARF6 has a critical role in regulating the shedding of microvesicles containing functional proteases. Microvesicle release is dependent on PLD activity, which in turn leads to the activation of ERK. ERK phosphorylates and activates MLCK, a known substrate for phospho-ERK. MLCK, in turn, phosphorylates and activates MLC. This would allow acto-myosin based contraction at the necks of microvesicles, facilitating their release into the extracellular space.

There is mounting evidence that the release of microvesicles serves to facilitate ECM degradation. Most striking in this regard is the reported presence of proteaseloaded membrane microvesicles with invasive properties in malignant ovarian ascites derived from women with stage I–IV ovarian cancer [14]. The study also showed that late stage ascites had significantly more microvesicles than that in early stage disease, although the invasive ability of the microvesicles was about the same irrespective of the disease stage. These studies assert the physiological relevance and importance of the data described here. Indeed, we show that processed forms of MT1-MMP, a key mediator of pericellular proteolysis, are present in the microvesicles.

Besides facilitating ECM degradation, microvesicles have also been shown to promote the horizontal propagation of oncogenes among subsets of cancer cells [31]. Microvesicles shed from glioblastoma cells were shown to contain microRNAs in addition to angiogenic factors [32]. Studies also suggest that microvesicles enable the escape of tumors from immune surveillance thus promoting tumor cell survival [33]. Consistent with these findings, we observed that MHC-class I is contained within microvesicles. How cargo is directed to surface associated vesicles will require further investigation, although it appears that cargo contained and trafficked via ARF6-regulated endosomal pathways, i.e. MHC Class I and β1 integrin receptors and VAMP-3 [4] are delivered to the microvesicles. Microvesicles are devoid of VAMP-7 and Rab8, both of which have been implicated in MT1-MMP delivery to the cell surface [34, 35] and also of transferrin receptors, which also traffic through the ARF6 compartment in some cell types (reviewed in [4]). Thus, cargo appears to be selectively sorted into microvesicles at the cell surface. We suggest that vesicle shedding occurs at specific sites on the plasma membrane and is designed to release selected cellular components into the surrounding environment, particularly those involved in cell-matrix interactions and matrix degradation. Rab8 and VAMP-7-dependent likely facilitate pericellular proteolysis.

This study also supports the view that microvesicle release is accompanied by localized lipid scrambling and vesicle-mediated proteolysis requires the binding of integrin receptors to the ECM [36]. Localized lipid scrambling with PS externalization has also been shown to occur in other non-apoptotic processes such as myotube formation [37] and rapid modulation of the activity of signaling proteins at the surface of non-apoptotic lymphocytes [38].

Pharmacological inhibition of actin polymerization and myosin function prevents microvesicle release suggesting that outward fission likely occurs via an actin-myosin based process. We show that ARF6- dependent activation of ERK promotes MLCK phosphorylation and subsequent MLC phosphorylation, thereby facilitating actomyosin-based contraction at vesicle necks leading to microvesicle release. The intricate rigor of this regulation is manifest in the fact that when ARF6 activation is blocked, not only does ERK activation and ERK-regulated MLCK phosphorylation not ensue, but also PKC mediated phosphorylation and inactivation of MLC occurs as a consequence (figure 7). All of these observations support earlier findings that ARF6-induced ERK activation has a profound

effect on tumor cell invasion. ARF6-induced ERK activation is dependent on the accumulation of PA. PA could facilitate ERK recruitment to the cell surface as described above, but may also be required to modify the lipid environment to facilitate the recruitment of components of the ERK cascade such as Raf to the plasma membrane as previously documented [39, 40].

Invadopodia and microvesicles appear to be distinct structures. Cortactin, a bona fide component of invadopodia, is absent in microvesicles. While proteases at the invadopodia surface might represent a mechanism for local pericellular proteolysis at the leading/invading membrane edge, microvesicle release likely promotes more distant focal proteolysis and creation of an invasion path. It is possible that some tumor lines may exhibit both invasion mechanisms whereas in others one of these mechanisms may dominate. The formation of invadopodia and release of microvesicles, both, are dependent on ARF6-induced ERK activation (figure 7).

The shedding of membrane microvesicles is not restricted to pathological conditions and is also observed in normal physiological conditions. For example, microvesicles secreted by skeletal cells enable bone mineralization *in vivo* while microvesicles secreted by normal endothelial cells have been implicated in angiogenesis [41]. Microvesicles have also been shown to play a role in mRNA transfer in embryonic stem cells and possibly in viral packaging and delivery to the extracellular environment [12, 42] [36]. Thus, in addition to providing strategies for cancer therapeutics and diagnostics, knowledge about the mechanism of the microvesicle shedding may shed light on other events requiring plasma membrane budding.

EXPERIMENTAL PROCEDURES

Antibodies and Plasmids

The following antibodies (vendors in parentheses) were used in this study. Anti-neutralizing β1-integrin, AIIB2, (Developmental Studies Hybridoma Bank at the University of Iowa), anti Rab-8A and anti-Tsk5 (Santa Cruz), anti-MHC-class I (Serotec), anti-HA (Covance), anti-TfnR from Zymed, antibodies against phospho-MLC, phospho-ERK, total ERK, cortactin and cleaved caspase 3 (Cell Signaling), anti-α-tubulin antibody (Sigma), anti-GFP (Roche). The MT1-MMP antibody was from a gift from Dr. M.C. Rio (France). GFP-ERK (Addgene plasmid 14747) was from Addgene [43]. HA-tagged ARF6-N48I was kindly provided by Dr. Nicholas Vitale (Centre National de la Recherche Scientifique & Universite Louis Pasteur). Plasmids encoding GFP-VAMP3 and GFP-VAMP7 were a gift from Thiery Galli (IJM, Paris, France).

Cell Culture and Microvesicle Isolation

LOX, $LOX^{ARF6\text{-}GTP}$ and $LOX^{ARF6\text{-}GDP}$ cell lines were cultured as described [5]. Cells were seeded in tissue culture flasks at 50% confluency. Media was carefully removed from cells at approximately 80% confluence and centrifuged consecutively at 800g for 10 min, 2500g for 15 min and 10,000g for 30 min. Where indicated, this was followed by centrifugation of the supernatant at 100,000g for 1 hour. Isolated microvesicles were washed in PBS, lysed and protein content was estimated using the Bradford assay (BioRad).

Gelatin Zymography

Microvesicles isolated from the growth media were lysed in RIPA buffer and separated on SDS-PAGE gels containing gelatin to assess gelatinase activity, as previously described [44].

'In vitro' Degradation Assay

The gelatin degradation assay was as previously described[45]. Alternatively, isolated microvesicles were seeded and incubated on gelatin-coated coverslips for 6–8 hours.

Immunofluorescent Staining and Microscopy

Cultured cells /microvesicles plated on poly-l lysine coated or gelatin-coated glass coverslips were fixed and processed as described [5]. F-actin distribution was visualized by staining with rhodamine-phalloidin (Molecular Probes). Labeling of the cell surface with FITC-Annexin V was performed using the kit from Beckman-Coulter according to the manufacturer's protocol. Cells were fixed and where indicated, the surface was labeled for β1-integrin (without permeabilization) and processed for immunofluorescence microscopy. Cells visualized using Nikon microscope coupled to a Bio-Rad MRC 1024 scanning confocal 3 channel system.

Electron Microscopy (EM)

Conventional and whole mount electron microscopy was performed as described [46]. Briefly, cells grown on coverslips were fixed with 2.5% glutaraldehyde in 0.1M cacodylate buffer overnight and processed as described. For whole mount membrane preparations, the 100,000g and 10,000 g pellets were gently suspended in a small volume of PBS and deposited for 20 min on formvar-carbon coated EM grids and processed for EM.

Supplementary Material

Refer to Web version on PubMed Central for supplementary material.

Acknowledgments

We thank Dr. Oystein Fodstad (Norwegian Radium Hospital) for the LOX cell line, Dr. Holly Hoover for invaluable contribution to the generation of the ARF6 cell lines and Dr. Jogender S. Tushir for critical insight into the signaling pathway described. JC is a GLOBES-NSF and Lilly Foundation pre-doctoral fellow. This work was supported in part by a grant from the National Cancer Institute (CA115316) to CD-S.

REFERENCES

1. Chambers AF, Groom AC, MacDonald IC. Dissemination and growth of cancer cells in metastatic sites. Nat Rev Cancer. 2002; 2:563–572. [PubMed: 12154349]
2. Vega FM, Ridley AJ. Rho GTPases in cancer cell biology. FEBS Lett. 2008; 582:2093–2101. [PubMed: 18460342]
3. Egeblad M, Werb Z. New functions for the matrix metalloproteinases in cancer progression. Nat Rev Cancer. 2002; 2:161–174. [PubMed: 11990853]
4. D'Souza-Schorey C, Chavrier P. ARF proteins: roles in membrane traffic and beyond. Nat Rev Mol Cell Biol. 2006; 7:347–358. [PubMed: 16633337]
5. Muralidharan-Chari V, Hoover H, Clancy J, Schweitzer J, Suckow MA, Schroeder V, Castellino FJ, Schorey JS, D'Souza-Schorey C. ADP-ribosylation factor 6 regulates tumorigenic and invasive properties in vivo. Cancer Res. 2009; 69:2201–2209. [PubMed: 19276388]
6. Hu B, Shi B, Jarzynka MJ, Yiin JJ, D'Souza-Schorey C, Cheng SY. ADP-ribosylation factor 6 regulates glioma cell invasion through the IQdomain GTPase-activating protein 1-Rac1-mediated pathway. Cancer Res. 2009; 69:794–801. [PubMed: 19155310]
7. Hashimoto S, Onodera Y, Hashimoto A, Tanaka M, Hamaguchi M, Yamada A, Sabe H. Requirement for Arf6 in breast cancer invasive activities. Proc Natl Acad Sci U S A. 2004; 101:6647–6652. [PubMed: 15087504]
8. Morishige M, Hashimoto S, Ogawa E, Toda Y, Kotani H, Hirose M, Wei S, Hashimoto A, Yamada A, Yano H, Mazaki Y, Kodama H, Nio Y, Manabe T, Wada H, Kobayashi H, Sabe H. GEP100

links epidermal growth factor receptor signalling to Arf6 activation to induce breast cancer invasion. Nat Cell Biol. 2008; 10:85–92. [PubMed: 18084281]

9. Morel O, Toti F, Hugel B, Freyssinet JM. Cellular microparticles: a disseminated storage pool of bioactive vascular effectors. Curr Opin Hematol. 2004; 11:156–164. [PubMed: 15257014]
10. Ratajczak J, Wysoczynski M, Hayek F, Janowska-Wieczorek A, Ratajczak MZ. Membrane-derived microvesicles: important and underappreciated mediators of cell-to-cell communication. Leukemia. 2006; 20:1487–1495. [PubMed: 16791265]
11. Hugel B, Martinez MC, Kunzelmann C, Freyssinet JM. Membrane microparticles: two sides of the coin. Physiology (Bethesda). 2005; 20:22–27. [PubMed: 15653836]
12. Cocucci E, Racchetti G, Meldolesi J. Shedding microvesicles: artefacts no more. Trends Cell Biol. 2009; 19:43–51. [PubMed: 19144520]
13. Dolo V, D'Ascenzo S, Violini S, Pompucci L, Festuccia C, Ginestra A, Vittorelli ML, Canevari S, Pavan A. Matrix-degrading proteinases are shed in membrane vesicles by ovarian cancer cells in vivo and in vitro. Clin Exp Metastasis. 1999; 17:131–140. [PubMed: 10411105]
14. Graves LE, Ariztia EV, Navari JR, Matzel HJ, Stack MS, Fishman DA. Proinvasive properties of ovarian cancer ascites-derived membrane vesicles. Cancer Res. 2004; 64:7045–7049. [PubMed: 15466198]
15. Tague SE, Muralidharan V, D'Souza-Schorey C. ADP-ribosylation factor 6 regulates tumor cell invasion through the activation of the MEK/ERK signaling pathway. Proc Natl Acad Sci U S A. 2004; 101:9671–9676. [PubMed: 15210957]
16. Bowden ET, Onikoyi E, Slack R, Myoui A, Yoneda T, Yamada KM, Mueller SC. Co-localization of cortactin and phosphotyrosine identifies active invadopodia in human breast cancer cells. Exp Cell Res. 2006; 312:1240–1253. [PubMed: 16442522]
17. Fevrier B, Raposo G. Exosomes: endosomal-derived vesicles shipping extracellular messages. Curr Opin Cell Biol. 2004; 16:415–421. [PubMed: 15261674]
18. Dolo V, Ginestra A, Cassara D, Violini S, Lucania G, Torrisi MR, Nagase H, Canevari S, Pavan A, Vittorelli ML. Selective localization of matrix metalloproteinase 9, beta1 integrins, and human lymphocyte antigen class I molecules on membrane vesicles shed by 8701-BC breast carcinoma cells. Cancer Res. 1998; 58:4468–4474. [PubMed: 9766680]
19. Taraboletti G, D'Ascenzo S, Giusti I, Marchetti D, Borsotti P, Millimaggi D, Giavazzi R, Pavan A, Dolo V. Bioavailability of VEGF in tumor-shed vesicles depends on vesicle burst induced by acidic pH. Neoplasia. 2006; 8:96–103. [PubMed: 16611402]
20. Donaldson JG. Multiple roles for Arf6: sorting, structuring, and signaling at the plasma membrane. J Biol Chem. 2003; 278:41573–41576. [PubMed: 12912991]
21. Robertson SE, Setty SR, Sitaram A, Marks MS, Lewis RE, Chou MM. Extracellular signal-regulated kinase regulates clathrin-independent endosomal trafficking. Mol Biol Cell. 2006; 17:645–657. [PubMed: 16314390]
22. Tushir JS, D'Souza-Schorey C. ARF6-dependent activation of ERK and Rac1 modulates epithelial tubule development. Embo J. 2007; 26:1806–1819. [PubMed: 17363898]
23. Nekhoroshkova E, Albert S, Becker M, Rapp UR. A-RAF kinase functions in ARF6 regulated endocytic membrane traffic. PLoS One. 2009; 4:e4647. [PubMed: 19247477]
24. Jovanovic OA, Brown FD, Donaldson JG. An effector domain mutant of Arf6 implicates phospholipase D in endosomal membrane recycling. Mol Biol Cell. 2006; 17:327–335. [PubMed: 16280360]
25. Sobieszek A, Strobl A, Ortner B, Babiychuk EB. Ca(2+)-calmodulin-dependent modification of smooth-muscle myosin light-chain kinase leading to its co-operative activation by calmodulin. Biochem J. 1993; 295(Pt 2):405–411. [PubMed: 8240237]
26. Klemke RL, Cai S, Giannini AL, Gallagher PJ, de Lanerolle P, Cheresh DA. Regulation of cell motility by mitogen-activated protein kinase. J Cell Biol. 1997; 137:481–492. [PubMed: 9128257]
27. Nguyen DH, Catling AD, Webb DJ, Sankovic M, Walker LA, Somlyo AV, Weber MJ, Gonias SL. Myosin light chain kinase functions downstream of Ras/ERK to promote migration of urokinase-type plasminogen activator-stimulated cells in an integrin-selective manner. J Cell Biol. 1999; 146:149–164. [PubMed: 10402467]

28. Goldberg PL, MacNaughton DE, Clements RT, Minnear FL, Vincent PA. p38 MAPK activation by TGF-beta1 increases MLC phosphorylation and endothelial monolayer permeability. Am J Physiol Lung Cell Mol Physiol. 2002; 282:L146–L154. [PubMed: 11741826]
29. Bogatcheva NV, Verin AD, Wang P, Birukova AA, Birukov KG, Mirzopoyazova T, Adyshev DM, Chiang ET, Crow MT, Garcia JG. Phorbol esters increase MLC phosphorylation and actin remodeling in bovine lung endothelium without increased contraction. Am J Physiol Lung Cell Mol Physiol. 2003; 285:L415–L426. [PubMed: 12740219]
30. Obara K, Ito Y, Shimada H, Nakayama K. The relaxant effect of okadaic acid on canine basilar artery involves activation of PKCalpha and phosphorylation of the myosin light chain at Thr-9. Eur J Pharmacol. 2008; 598:87–93. [PubMed: 18835557]
31. Al-Nedawi K, Meehan B, Micallef J, Lhotak V, May L, Guha A, Rak J. Intercellular transfer of the oncogenic receptor EGFRvIII by microvesicles derived from tumour cells. Nat Cell Biol. 2008; 10:619–624. [PubMed: 18425114]
32. Skog J, Wurdinger T, van Rijn S, Meijer DH, Gainche L, Sena-Esteves M, Curry WT Jr, Carter BS, Krichevsky AM, Breakefield XO. Glioblastoma microvesicles transport RNA and proteins that promote tumour growth and provide diagnostic biomarkers. Nat Cell Biol. 2008; 10:1470–1476. [PubMed: 19011622]
33. Valenti R, Huber V, Iero M, Filipazzi P, Parmiani G, Rivoltini L. Tumor-released microvesicles as vehicles of immunosuppression. Cancer Res. 2007; 67:2912–2915. [PubMed: 17409393]
34. Bravo-Cordero JJ, Marrero-Diaz R, Megias D, Genis L, Garcia-Grande A, Garcia MA, Arroyo AG, Montoya MC. MT1-MMP proinvasive activity is regulated by a novel Rab8-dependent exocytic pathway. Embo J. 2007; 26:1499–1510. [PubMed: 17332756]
35. Steffen A, Le Dez G, Poincloux R, Recchi C, Nassoy P, Rottner K, Galli T, Chavrier P. MT1-MMP-dependent invasion is regulated by TI-VAMP/VAMP7. Curr Biol. 2008; 18:926–931. [PubMed: 18571410]
36. Freyssinet JM. Cellular microparticles: what are they bad or good for? J Thromb Haemost. 2003; 1:1655–1662. [PubMed: 12871302]
37. van den Eijnde SM, van den Hoff MJ, Reutelingsperger CP, van Heerde WL, Henfling ME, Vermeij-Keers C, Schutte B, Borgers M, Ramaekers FC. Transient expression of phosphatidylserine at cell-cell contact areas is required for myotube formation. J Cell Sci. 2001; 114:3631–3642. [PubMed: 11707515]
38. Elliott JI, Surprenant A, Marelli-Berg FM, Cooper JC, Cassady-Cain RL, Wooding C, Linton K, Alexander DR, Higgins CF. Membrane phosphatidylserine distribution as a non-apoptotic signalling mechanism in lymphocytes. Nat Cell Biol. 2005; 7:808–816. [PubMed: 16025105]
39. Andresen BT, Rizzo MA, Shome K, Romero G. The role of phosphatidic acid in the regulation of the Ras/MEK/Erk signaling cascade. FEBS Lett. 2002; 531:65–68. [PubMed: 12401205]
40. Hong JH, Oh SO, Lee M, Kim YR, Kim DU, Hur GM, Lee JH, Lim K, Hwang BD, Park SK. Enhancement of lysophosphatidic acid-induced ERK phosphorylation by phospholipase D1 via the formation of phosphatidic acid. Biochem Biophys Res Commun. 2001; 281:1337–1342. [PubMed: 11243883]
41. Taraboletti G, D'Ascenzo S, Borsotti P, Giavazzi R, Pavan A, Dolo V. Shedding of the matrix metalloproteinases MMP-2, MMP-9, and MT1-MMP as membrane vesicle-associated components by endothelial cells. Am J Pathol. 2002; 160:673–680. [PubMed: 11839588]
42. Ratajczak J, Miekus K, Kucia M, Zhang J, Reca R, Dvorak P, Ratajczak MZ. Embryonic stem cell-derived microvesicles reprogram hematopoietic progenitors: evidence for horizontal transfer of mRNA and protein delivery. Leukemia. 2006; 20:847–856. [PubMed: 16453000]
43. Yung Y, Yao Z, Aebersold DM, Hanoch T, Seger R. Altered regulation of ERK1b by MEK1 and PTP-SL and modified Elk1 phosphorylation by ERK1b are caused by abrogation of the regulatory C-terminal sequence of ERKs. J Biol Chem. 2001; 276:35280–35289. [PubMed: 11463794]
44. Manicourt DH, Lefebvre V. An assay for matrix metalloproteinases and other proteases acting on proteoglycans, casein, or gelatin. Anal Biochem. 1993; 215:171–179. [PubMed: 8122775]
45. Hoover H, Muralidharan-Chari V, Tague S, D'Souza-Schorey C. Investigating the role of ADP-ribosylation factor 6 in tumor cell invasion and extracellular signal-regulated kinase activation. Methods Enzymol. 2005; 404:134–147. [PubMed: 16413265]

46. Raposo G, Nijman HW, Stoorvogel W, Liejendekker R, Harding CV, Melief CJ, Geuze HJ. B lymphocytes secrete antigen-presenting vesicles. J Exp Med. 1996; 183:1161–1172. [PubMed: 8642258]

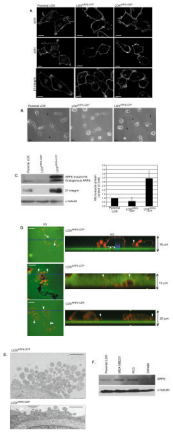

Figure 1. Phenotypic variations observed in LOX$^{ARF6\text{-}GDP}$ and LOX$^{ARF6\text{-}GTP}$ mutant lines

(A) Parental LOX, LOX$^{ARF6\text{-}GTP}$ and LOX$^{ARF6\text{-}GDP}$ cells lines were fixed and stained with rhodamine phalloidin to visualize actin filament distribution or β1-integrin antibody, as indicated. Panels show the range of phenotypes in the LOX cell lines. Bar: 10μm. **(B)** Parental LOX, LOX$^{ARF6\text{-}GTP}$ and LOX$^{ARF6\text{-}GDP}$ cells in culture at low confluency were imaged using phase-contrast microscopy. Arrows point to shed vesicles in the growth media of LOX and LOX$^{ARF6\text{-}GTP}$ cells. Bar: 10μm. **(C)** Vesicles released into the growth media from 2.2 × 10^6 LOX, LOX$^{ARF6\text{-}GTP}$ and LOX$^{ARF6\text{-}GDP}$ cells, were isolated and probed for ARF6 and β1 integrin by western blotting (left) or protein was quantitated (right). Cell lysates were probed for ARF6 and α-tubulin by western blotting. Lower and higher molecular weight ARF6 bands in LOX^{ARF6} cells correspond to endogenous and HA-tagged exogenous ARF6 respectively. **(D)** LOX$^{ARF6\text{-}GTP}$ and LOX$^{ARF6\text{-}GDP}$ cells were plated on FITC-gelatin-coated coverslips and allowed to invade. The cells were fixed and stained for cortactin (blue) and actin (red) (upper panel), or β1 integrin (red) (middle and lower panels). Arrows point to invadopodia and arrowheads indicate shed vesicles. Note arborization phenotype of LOX$^{ARF6\text{-}GTP}$ cells when the underlying gelatin is relatively thick (middle panel). Bar: 10μm. **(E)** LOX$^{ARF6\text{-}GTP}$ and LOX$^{ARF6\text{-}GDP}$ cells lines were analyzed by electron microscopy. Image in top panel shows heterogeneous vesicular structures near the surface of LOX$^{ARF6\text{-}GTP}$ cells. Lower panel shows vesicular structures that appear to stud the surface of LOX$^{ARF6\text{-}GDP}$ cells. Bar: 1000nm. **(F)** Vesicles released into the growth media from an equivalent number (1.5 × 10^6 cells) of indicated tumor cells lines in culture were isolated and probed for ARF6 by western blotting.

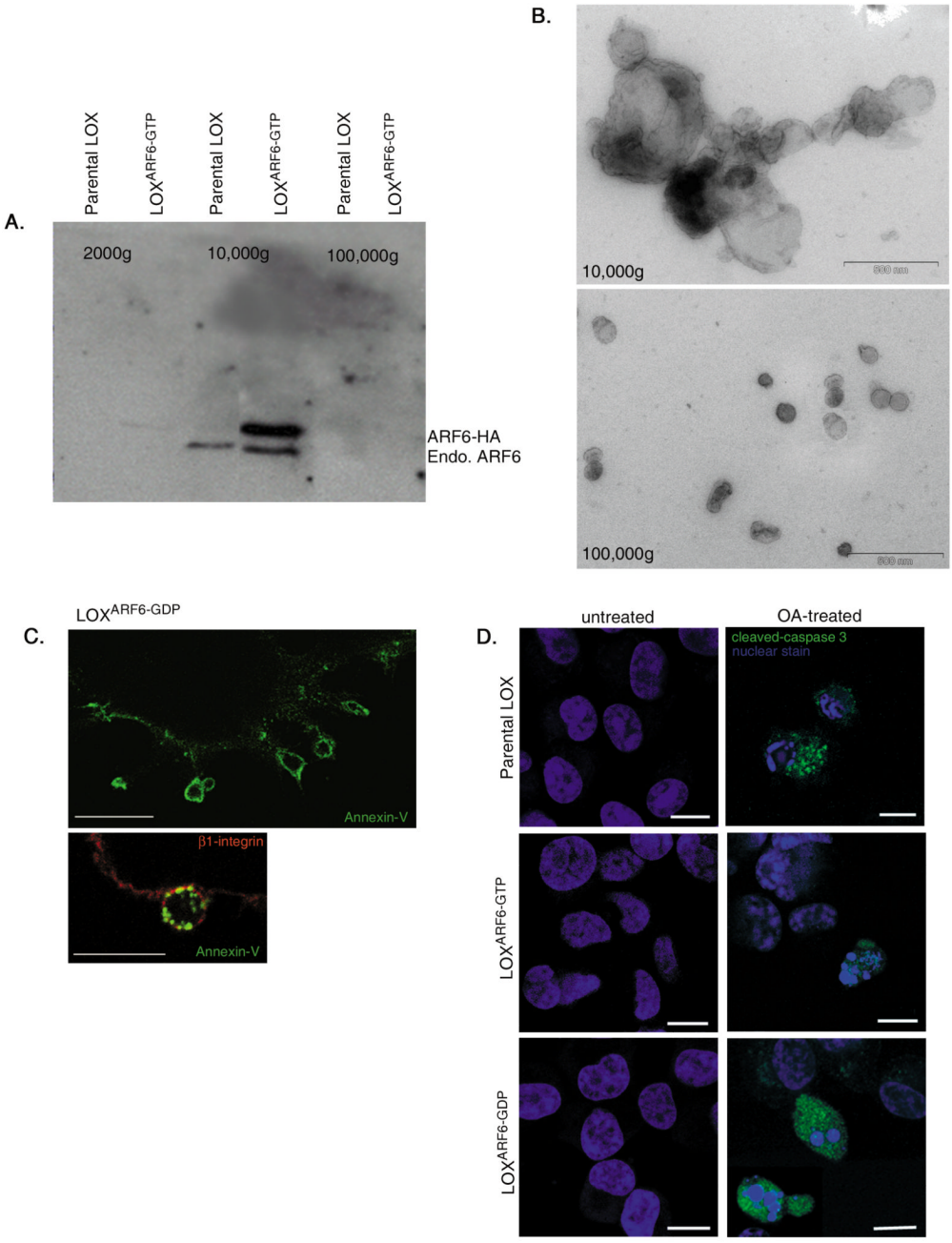

Figure 2. ARF6-positive microvesicles are distinct from exosomes

(A) Microvesicles shed by parental LOX and LOX$^{ARF6\text{-}GTP}$ cell lines were fractionated as described in methods and equivalent protein from each fraction was probed for ARF6. Endogenous ARF6 and HA-tagged mutant ARF6 are enriched only in the 10,000g fraction. **(B)** Fractionated vesicle populations isolated from LOX$^{ARF6\text{-}GTP}$ cells were analyzed by whole mount electron microscopy. Microvesicles isolated in the 10,000g fraction are larger (300 – 900nm) and heterogeneous relative to the more uniform 50–70nm vesicles in the 100,000g fraction typical of exosomes. Bar: 500nm. **(C)** The surface of LOX$^{ARF6\text{-}GDP}$ cells was labeled with Annexin V (green) to demarcate areas of PS externalization, and for β1-integrin (red), a surface marker. Top panel shows Annexin V labeling only. When the green

signal is dampened, enrichment of Annexin V labeling at sites of vesicle shedding is observed. Bar: 10μm. (**D**) Parental LOX, $LOX^{ARF6\text{-}GDP}$ and $LOX^{ARF6\text{-}GTP}$ cell lines with or without treatment with 50nM okadaic acid for 3hrs, were fixed and labeled for cleaved caspase-3 (green) and stained with topro-3-iodide, a nuclear stain (blue). Scale bar: 10μm.

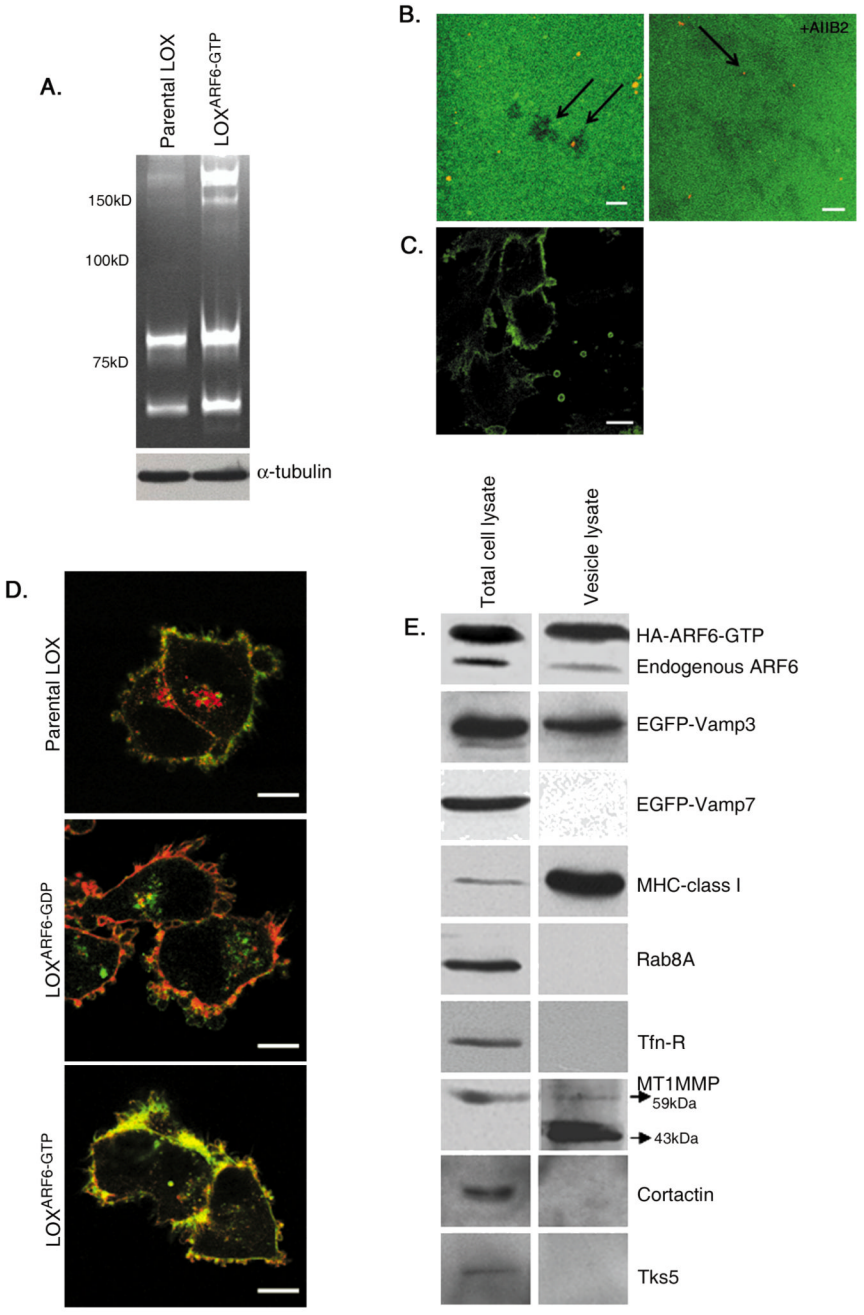

Figure 3. Shed microvesicles contain functional proteases and other selective membrane proteins

(A) Microvesicles shed from an equal number of parental LOX and LOX$^{ARF6\text{-}GTP}$ cells were isolated, and microvesicle lysates were analyzed by gelatin zymography. Cell lysates were probed for α-tubulin expression. High and low molecular weight gelatinases are present in microvesicle lysates. **(B)** Shed microvesicles isolated from the growth medium were gently overlaid on FITC-gelatin-coated glass coverslips for 8 hours in the absence or presence of AIIB2, the anti-β1-integrin blocking antibody. Coverslips were stained for actin (red) to identify microvesicles (see arrows). The dark spots on the FITC-gelatin are indicative of degradation underneath isolated microvesicles (left panel). Adhesion of microvesicles to the matrix was reduced to less than 10% in the presence of AIIB2 antibody.

Image intentionally shows residual labeling (right panel). Bar: 10μm. **(C)** Non-permeablized $LOX^{ARF6\text{-}GTP}$ cells were labeled with β1-integrin antibody to label the extracellular surface. Bar: 10μm. **(D)** Parental LOX, $LOX^{ARF6\text{-}GDP}$ and $LOX^{ARF6\text{-}GTP}$ cells were fixed and stained for actin (green) and endogenous MHC-1 (red). Bar: 10μm. **(E)** Lysates of $LOX^{ARF6\text{-}GTP}$ cells or of shed microvesicles were analyzed for indicated endogenous proteins or transfected proteins (EGFP-VAMP3 or EGFP-VAMP7) by western blotting.

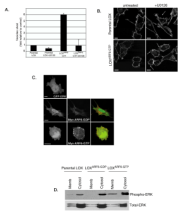

Figure 4. Microvesicle shedding requires ERK signaling

(A) Parental LOX and LOX$^{ARF6\text{-}GTP}$ lines were treated with 30μM U0126 and microvesicles shed into the media were isolated and quantitated for protein. Data from 5 independent experiments is shown. Bar: 10μm. **(B)** Parental LOX and LOX$^{ARF6\text{-}GTP}$ cell lines with or without treatment with U0126 were fixed and stained for actin. Arrows point to the microvesicles at the cell surface. **(C)** GFP-ERK (green) and Myc-tagged-ARF6 mutants as indicated (red) were transiently transfected into LOX, fixed and stained with anti-Myc. There is overlap of GFP-ERK and ARF6-GDP in endosomes and a significant ERK pool is at the cell surface with ARF6-GTP expression. Bar: 10μm. **(D)** Parental LOX, LOX$^{ARF6\text{-}GDP}$ and LOX$^{ARF6\text{-}GTP}$ were subjected to subcellular fractionation and the amount of endogenous phospho-ERK and total-ERK in the membrane and cytosolic fractions were analyzed by immunoblotting.

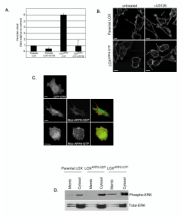

Figure 5. ARF6-induced ERK activation requires PLD

(A) Lysates of LOX cells transiently transfected with HA-tagged-ARF6-N48I mutant, were probed for phospho-ERK and total ERK by western blotting. The data is representative of 3 separate experiments. Band intensities were quantified by densitometry and the ratio of phospho-ERK to total ERK is shown. **(B)** Microvesicles released into the media by parental LOX and LOX cells transfected with ARF6-N48I were isolated by differential centrifugation, quantitated for the protein content and the data is shown. Microvesicles in the growth media of cells expressing ARF6-N48I is lower relative to untransfected controls. **(C)** LOX cells were cotransfected with expression plasmids encoding ARF6-N48I and GFP-Spo20-PABD, a fluorescent PA probe. PA levels are decreased upon expression of the ARF6 mutant. **(D)** LOX cells were treated with 0.3% t-butanol or 1-butanol for 30 min, fixed and stained for actin to visualize surface-associated microvesicles. For each experimental condition, cells that showed eight or more microvesicles at the surface were scored, and the percent inhibition of vesicle shedding was determined. 250 cells were observed for each experiment and the data from four independent experiments is plotted. **(E)** Lysates of $LOX^{ARF6\text{-}GDP}$ cells treated with propranolol (0.1mM) and atenolol (10uM) were probed for phospho-ERK and total-ERK. Band intensities were quantified by densitometry. The data is representative of 3 independent experiments. **(F)** $LOX^{ARF6\text{-}GDP}$ cells treated with propranolol or atenolol were visualized and cells with microvesicles at the cell surface were scored as described above. Propranolol-treatment of $LOX^{ARF6\text{-}GDP}$ cells restored vesicle shedding.

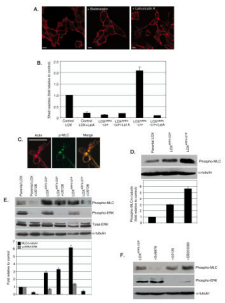

Figure 6. ERK-regulated microvesicle shedding requires MLCK-phosphorylation

(A) LOX cells were treated with either 100μM blebbistatin or 2μM Latrunculin A and fixed and stained for actin to visualize surface-associated microvesicles. Bar: 10μm. **(B)** Parental LOX, $LOX^{ARF6\text{-}GTP}$ and $LOX^{ARF6\text{-}GDP}$ cells in culture were incubated with fresh media containing 2μM Latrunculin A (Lat A) for 45 min. Microvesicles released were isolated, quantitated for protein and the data is shown. **(C)** LOX cells were fixed and stained for endogenous phospho-MLC (green) and actin (red). Note the localization of phospho-MLC at the 'necks' of surface microvesicles. Bar: 5μm. **(D)** Cell lysates of LOX, $LOX^{ARF6\text{-}GTP}$ and $LOX^{ARF6\text{-}GDP}$ cells lines were analyzed for endogenous phospho-MLC by western blotting. α-tubulin expression was also assessed as an indicator for equal loading. Band density was measured by densitometric scanning. **(E)** Lysates of LOX cells treated with U0126 (30uM) were analyzed for endogenous phospho-MLC, phospho-ERK, total-ERK and α-tubulin by western blotting. Additional lanes on the immunoblot between lanes 2 and 3 were spliced out. Band density was measured by densitometric scanning. **(F)** $LOX^{ARF6\text{-}GDP}$ cells were treated with various inhibitors; Go6976 (PKC inhibitor-10uM), ML-7 (MLCK inhibitor-10uM), U0126 (MEK inhibitor-30uM) and SB203580 (p38 inhibitor-10uM) for 2 hrs at 37°C. Cell lysates were probed for phospho-MLC, phospho-ERK and α-tubulin by western blotting.

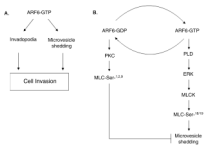

Figure 7. Working model for ARF6-mediated regulation of cell invasion

A. Activated ARF6 facilitates tumor cell invasion by promoting invadopodia formation and microvesicle shedding. The formation of invadopodia and microvesicle release requires ARF6 and ERK. **B.** The signaling pathway downstream of ARF6-regulated ERK activation required for microvesicle shedding is shown on the right. ARF6-regulated ERK localization to and its activation at plasma membrane require PLD. ERK-induced phosphorylation of MLCK in turn, promotes MLC phosphorylation required for actomyosin-based membrane fission leading to microvesicle release.